Tikrit Journal of Engineering Sciences

TJES Tikrit Journal of Engineering Sciences

Open Access

Article

Groundwater Steady Flow Simulation in the Confined Aquifer of the Lower Zab River Basin, Iraq

Mohammed Jallel AL Janabi*, **Ruqayah Kadhim Mohammed**

Civil Department, Engineering College, Babylon University, Babil, Iraq.

Emails:
Mohammed Jallel AL Janabi: moh_82eng@yahoo.com, Ruqayah Kadhim Mohammed: r.mohammed1@yahoo.com

Abstract:

There is a freshwater deficit and growing groundwater dependence in many regions of Iraq due to population development and increased water demand for numerous uses. The water table declines due to the area's numerous deep wells drilled randomly and a constant increase in water pumping from groundwater reserves. Thus, it is vital to evaluate the water resource management. The present research examines the potential for degradation and the stressors affecting the confined aquifer of the Lower Zab watershed across the governorates of Kirkuk, Erbil, and Sulaymaniyah. Utilizing the Groundwater Modelling System (GMS V10.7) software, a numerical simulation of groundwater flow was conducted to model the basin's confined aquifer. The steady-state calibration results revealed a hydraulic conductivity (HK) ranging from 3 to 10 m/day, while the estimated recharge rate (RH) was 0.0004 m/day. The model was calibrated for each observation well in the watershed by comparing observed and simulated groundwater heads. The most sensitive parameters identified were conductance (for rivers and reservoirs), HK, and RH, with the lowest residual determined for these factors. Assessment of the model's reliability utilized the root mean square error (RMSE), mean absolute error (MAE), and mean error (ME). The estimate's standard error is 0.6259 m; its RMSE is approximately 3.531 m; its NRMS is -3.352; and its maximum and minimum residuals are 5.532 m in well number W_8 and -7.254 m in well number W_4, respectively. Its residual mean and absolute residual mean are -1.053 m and 2.982 m, respectively. The comparison results have a correlation coefficient of 0.99. Acknowledging the lack of prior research, the study aimed to fill this gap by developing a comprehensive model that could significantly advance knowledge and management of the area's groundwater resources. The study sought to provide crucial insights for efficient planning and sustainable groundwater development in the Lower Zab Basin by establishing a fundamental groundwater flow model.

Keywords:

Groundwater modelling, GMS, Lesser Zab River, Modflow, Steady state.

Highlights:

- Modelling Groundwater with the GMS Modflow program.
- Recharge and Hydraulic conductivity were computed in an inverse model tool (PEST).
- The Head Counter Map was done for the study area.

Article History:

Received:	21	Jul.	2024
Received in revised form:	07	Dec.	2024
Accepted:	02	Feb.	2025
Final Proofreading:	14	Mar.	2026
Available online:	26	Apr.	2026

https://doi.org/10.25130/tjes.33.1.3

Corresponding Author*:

Mohammed Jallel AL Janabi
Civil Department, Engineering College, Babylon University, Babil, Iraq.
Email: moh_82eng@yahoo.com

Citation:

AL Janabi MJ, Mohammed RK. **Groundwater Steady Flow Simulation in the Confined Aquifer of the Lower Zab River Basin, Iraq**. *Tikrit Journal of Engineering Sciences* 2026; **33**(1): 2274.

1.INTRODUCTION

Only a minor portion of the river valleys use the water from the Tigris and Euphrates rivers and their tributaries. Groundwater is a crucial water source in Iraq, particularly in dry and semiarid regions, serving vital functions such as providing water for drinking, irrigation, and industrial use [1]. The Tigris and its tributaries primarily flow through a narrow zone along the river valleys in the northeastern region of Iraq, which experiences low annual rainfall and frequent droughts, posing a significant global concern. Iraq has numerous divided watersheds and a variety of natural depressions that serve as watersheds for the Tigris and Euphrates rivers. It is situated in the country downstream of these rivers. The water balance technique is a primary approach in hydrology used to address crucial theoretical and practical hydrological issues [2]. In recent decades, there has been increasing pressure on surface water resources globally due to issues, such as climate change, population growth, and the deterioration of historical water sources. It is essential to reconcile the available future water supply with the projected increase in demand to ensure a reliable water supply for various stakeholders and purposes, including domestic, agricultural, industrial, and energy needs [3]. In many cities worldwide, groundwater has become the primary source of water. Groundwater, existing at various depths in the subsurface and spanning large areas, requires protection from surface contaminants to maintain its quality for diverse uses [4]. Groundwater modelling plays a significant role in understanding the behavior of groundwater flow systems through observation and prediction, thus contributing to long-term groundwater resource management. Consequently, groundwater modelling is integral to most groundwater protection, development, and enhancement projects [5]. Numerous researchers have focused on groundwater modelling. For instance, Mustafa et al. [6] conducted studies to map groundwater levels in the Erbil basin, employing two popular interpolation methods, Kriging and IDW, from 2004 to 2022. The results successfully indicated a significant decrease in groundwater tables over these 18 years, by approximately 46.86 m. Mohammed and Scholz [7] introduced a novel model that integrates the Eckhardt algorithm flow, the duration curve, and the Chapman filtering algorithm for the lower Zab River basin in northern Iraq over the period 1998–2008. According to their analysis, precipitation events impact some subsurface water. Al-Gburi et al. [8] conducted studies examining the stable isotope composition in groundwater of the Shawn sub-basin, Kirkuk, northeast of Iraq, in 2020 and 2021. Their findings indicated that the estimated groundwater recharge, based on weighted oxygen isotopes, accounts for approximately 9.2% of the annual rainfall. The low recharge value contributes to dry water conditions [8]. In a separate study, ALSlevani and ALMohsen [9] utilized MODFLOW to analyze groundwater by building a conceptual groundwater model in the province of Nineveh. The study demonstrated that conceptual models could effectively represent a groundwater system and provide insights into predicting groundwater changes under various pumping scenarios. Lastly, Ta'any et al. [10] investigated groundwater management using the MODFLOW model in the Jerash catchment area, Jordan. Their model revealed that approximately 23 MCM/year seeps into the lower aquifer, while 21 MCM/year flows out as lateral flow and natural spring discharge. Furthermore, an additional 2–3 MCM/year flows into the aquifer layer as lateral flow alongside vertical recharge from the upper layer. Over 25 MCM/year flows out of the aquifer as lateral flow and spring discharge [10]. Baghel et al. [11] conducted a detailed investigation of groundwater flow in the upper Seonath basin, a subbasin of the Mohanadi River in India. They developed a groundwater flow budget model and found that approximately 1,200,000 m^3 of water is extracted daily before the monsoon season. The recharge from the stream and storage sustains the water inflow in the area, and the constant head is sufficient to support a continuous abstraction of 2000 m^3 per day. In a separate study, Marios [12] examined the simulation of groundwater flow in the alluvial aquifer of the Korisos basin in NW Greece using the Modflow code. The groundwater flows northeast to southwest towards the Kastoria lake, with a mean hydraulic gradient (i) of 1.5×10^{-3}. The storage coefficient (S) ranged from 1.9×10^{-4} to 9.3×10^{-3}, the transmissivity (T) ranged from 1.4×10^{-3} to 1×10^{-2} m^2/s, and the average HK was measured at 6.7×10^{-5} m/s. The MODFLOW code, in conjunction with GMS 7.1, was successfully applied to the quaternary deposits of the area under steady-state conditions. Model calibration was successful, as evidenced by the deviations between the calculated and observed head values and the RMSE of roughly 0.61 m. According to the Ministry of Water Resources, the National Statistics Center reports, surface water entering the Lower Zab River decreased from an estimated 11.56 billion cubic meters (BCM) in 2014 to a predicted 4.29 BCM in 2020. Additionally, the amount of water extracted from wells increased to 73,474 m^3 per day in Kirkuk Governorate alone. That is because most previous studies focused on the region's groundwater quality, while few examined the water balance, contour maps of groundwater level, the hydraulic conductivity of water reservoirs, and recharge replenishing

groundwater. In addition to determining accurate drilling locations and the effects of hydraulic conductivity on well depletion and continuity, the study aimed to present a thorough picture of groundwater levels. Furthermore, it facilitates the best possible management of surface and groundwater scarcity, thereby lessening the effects of climate change and helping overcome its aftereffects. Acknowledging the lack of prior research, the study aimed to fill this gap by developing a comprehensive model that could significantly advance knowledge and management of the area's groundwater resources. By developing a basic groundwater flow model, the study aimed to offer vital insights for effective planning and sustainable groundwater development in the Lower Zab Basin. The lack of prior studies highlighted the significance of this study, making it a trailblazing attempt to fill key information gaps about groundwater in this specific geographic setting. The present study aims to create a contour map of piezometric heads and to assess the hydraulic characteristics of a confined aquifer in the Lower Zab geological formation in northeastern Iraq, which includes the governorates of Kirkuk, Erbil, and Sulaymaniyah. These characteristics include the HK and RH, which can be determined through numerical modelling using the MODFLOW package alongside the GMS program.

2.MATERIALS AND METHODS

2.1.Study area location, Tectonic Setting, and Stratigraphy

The Lesser Zab River Basin is situated between latitudes 43° 21′ 41"–46° 17′ 55" N and 35° 1′ 29"–36° 54′ 41" E. The greater part of the Lesser Zab River lies in the northeast region of Iraq, while the lesser part lies in Iran, as shown in Fig. 1 (A-D). With a total surface area of 19700.845 km², 25.23% of the basin is located inside Iran (4970.310 km²), and 74.77% is located inside Iraq (14729.690 km²).

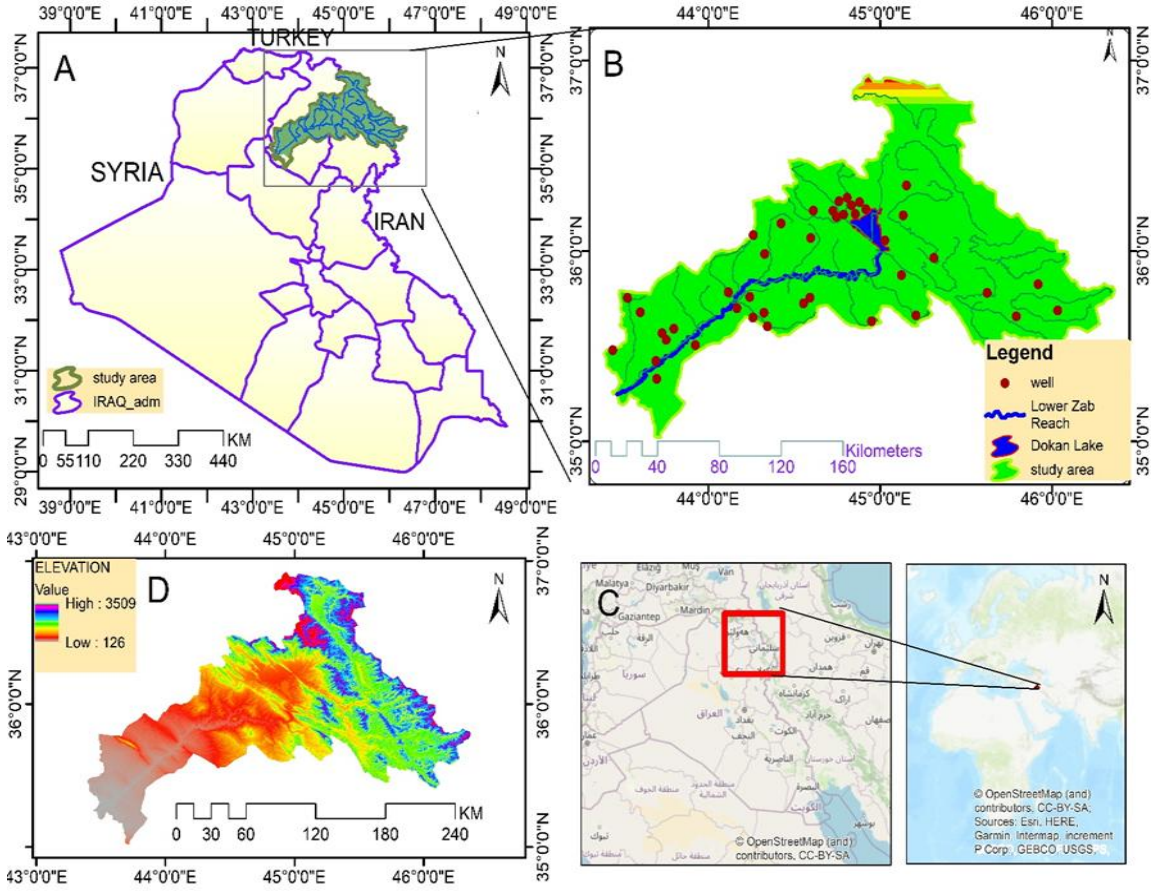

Fig. 1 (A) Location Map of the Lower Zab River Basin in Iraq, (B) Boundaries of the Basin and Hydraulic Parameters, (C) Digital Elevation Model of the Lower Zab River Region, where it is in Iraq, and (D) Location on the World Map.

The topographic characteristics of the study area, such as elevation accuracy of 30 m and the specific SRTM version, were obtained from the US Geological Survey (USGS) (http://earthexplorer.usgs.gov). The last map used to verify the watershed shape was created by removing the surrounding areas in ArcMap software, as shown in Fig. 1 (D). Based on its topography, the watershed can be categorized into two main sections: a flat, gently sloping area and a hilly region [13]. The geomorphologic units, comprised of seven genetic classes, encompass a variety of lithomorphologic landforms. Geologic

structures, tectonics, and climatic factors all affect the weathering, erosion, and deposition processes that shape these units [14]. The concluding stage of vigorous orogenic activity, which transpired during the Late Miocene and Pliocene and peaked in the Early Pleistocene, greatly influenced the geomorphological development of the basin. The final inclined strata affected by this intense activity date back to the Pliocene Early Pleistocene Formation, with the tilted beds of the historic Tigris River terraces as a remarkable illustration. However, the presence of horizontally arranged beds indicates that tectonic activity continued during the Quaternary Period, albeit at a relatively low intensity. This tectonic activity and associated structures significantly influenced the development of the primary geomorphologic units and the surface relief of the affected area [13]. During the Quaternary Period, climate significantly influenced the regulation of geomorphic processes, such as weathering, erosion, and fluvial processes, as well as lithologic, topographic, and structural factors. Cyclical pluvial and interpluvial climatic phases indicate long-term Quaternary climate changes in semiarid regions [1]. Due to the Lower Zab River Basin's heavy reliance on groundwater, its movement is crucial. According to data from the National Center for Statistics, Kirkuk's average daily groundwater withdrawal for processing is 73 m^3, and this amount has decreased as processing on the Little Zab River has decreased. According to data, the supply from the Kirkuk Irrigation Canal would drop from 1.76 billion cubic meters (BCM) per second in 2022 to 1.55 BCM annually in 2022, increasing demand and necessitating addressing the groundwater deficit. The Dukan Dam's storage percentage and the Dukan station's 50% reduction in rainwater are similar. The quantity of evaporation from the Dokan Lake reservoir grew from 2.44 BCM in 2022 to 2.23 BCM in 2021, and it reached 230.57 million cubic meters in the water year 2021 to 2022.

2.2.Data Availability and Collected

The parameters specified in the input files for the groundwater flow process can be utilized to compute most model inputs. These inputs encompass model layers, hydraulic conductivities in both horizontal and vertical directions, anisotropies in both horizontal and vertical directions, specific storage, specific yield, head boundaries, area recharge rate, evapotranspiration, and constant head boundaries. Forty-four observations and pumping wells, detailed in Table 1, were employed to establish the model, involving coordinating the model with UTM "WGS-84" and gathering water-surface level data, discharge, hydraulic conductivity, and transmissivity for each well to identify head equipotential within the study area. Furthermore, the data were utilized to gauge increases and decreases along head-dependent boundaries, such as rivers, and to measure flow through constant-head boundaries. To develop the groundwater model, a comprehensive set of hydrogeological and geological data was compiled. This data entailed gathering information on surface and subsurface geology, the water table, precipitation, evapotranspiration, pumped abstraction, stream flows, boundary conditions, hydraulic properties, geological formations, lithological descriptions, and a topographic map with drilling and observation well locations.

Table 1 The Discharge Wells Used in The Simulation, UTM (Zone: 38 (42°E - 48°E - Northern Hemisphere)), WGS84 System.

No.	Long[1]	Lat[2]	Q[3]	K[4]	T[5]	No.	Long[1]	Lat[2]	Q[3]	K[4]	T [5]
W_1	44.34	35.60	194	1.2	59	W_{23}	44.16	35.7	736	3	302
W_2	43.44	35.47	194	1.2	35	W_{24}	45.02	36.05	778	0.3	30
W_3	44.82	36.19	257	1.3	65	W_{25}	43.7	35.32	778	0.5	32
W_4	43.8	35.59	324	0.2	11	W_{26}	43.69	35.42	878	0.8	61
W_5	44.91	36.21	353	8.2	90	W_{27}	44.88	36.24	907	2.4	168
W_6	45.20	35.66	389	2	74	W_{28}	44.58	36.07	940	2.3	197
W_7	44.59	35.75	389	0.3	14	W_{29}	43.75	35.53	940	5.1	91
W_8	43.73	35.56	396	3.5	153	W_{30}	44.73	36.24	950	5.2	430
W_9	43.92	35.50	455	1.7	67	W_{31}	44.74	36.17	990	1.9	148
W_{10}	44.26	36.08	528	0.9	61	W_{32}	44.11	35.78	990	7.4	141
W_{11}	44.61	36.21	583	0.3	13	W_{33}	44.72	36.21	1166	2.9	239
W_{12}	44.81	36.27	594	0.9	59	W_{34}	44.78	36.19	1296	5.1	290
W_{13}	44.76	36.26	594	0.2	38	W_{35}	44.83	36.20	1296	18	276
W_{14}	44.42	36.14	594	0.4	26	W_{36}	44.32	35.67	1510	3.6	282
W_{15}	44.83	36.21	627	7.7	441	W_{37}	44.83	36.19	1555	10.8	864
W_{16}	44.78	36.25	648	5.5	430	W_{38}	44.80	36.28	1642	5.9	433
W_{17}	44.88	36.25	648	0.4	27	W_{39}	44.95	35.63	1642	0.7	74
W_{18}	44.83	36.24	648	4.4	351	W_{40}	44.59	36.06	1782	1.8	157
W_{19}	44.55	35.72	648	0.6	22	W_{41}	44.84	36.21	1918	6.7	571
W_{20}	44.82	36.21	660	4.3	150	W_{42}	44.85	36.19	1944	7.3	601
W_{21}	43.53	35.75	660	0.6	36	W_{43}	44.26	35.64	2742	1.9	179
W_{22}	44.85	36.22	726	0.4	31	W_{44}	44.24	35.75	3240	7.5	255

[1]Longitud (°); [2]Latitude (°); [3]Discharge (m^3/day); [4]Hydrulic conductivity (m/day); [5]Transmissivity (m^2/day).

2.3.Groundwater Modelling

The study area is modeled as a confined single-layer aquifer. A total of ten thousand horizontal grid cells, or 100 (x) × 100 (y) discretization, were employed for this study. The surface layer was established using digital elevation data from the SRTM 30. Despite sediment accumulation across the region, a continuum approach is considered applicable. Therefore, the Darcy equation can be utilized to model and elucidate groundwater flow. Equal grid spacing was selected for the finite-difference technique. As geophysical data are lacking, the aquifer's bottom elevation cannot be determined, so a constant value for each cell was employed as a fundamental assumption. The governing equation for transient 3D GW flow in heterogeneous, anisotropic porous media with a constant density non-equilibrium is expressed mathematically as follows [2]:

$$\frac{\partial}{\partial x}\left(K_x\frac{\partial h}{\partial x}\right)+\frac{\partial}{\partial y}\left(K_y\frac{\partial h}{\partial y}\right)+\frac{\partial}{\partial z}\left(K_z\frac{\partial h}{\partial z}\right)\pm W=S_s\frac{\partial h}{\partial t} \quad (1)$$

where K_x, K_y, and K_z (LT^{-1}) represent the hydraulic conductivity values along the x, y, and z coordinates, respectively, assumed to be the principal directions of anisotropy [2]. Here, h (L) stands for the hydraulic head of the fluid, W denotes water sources/sinks as well as being a volumetric flux per unit volume, and S_s (L^{-1}) signifies porous media-specific storage, while t (T) represents the time scale. In the case of a homogenous, isotropic medium ($K_x = K_y = K_z$), Eq. (1) simplifies to:

$$\frac{\partial^2 h}{\partial x^2}+\frac{\partial^2 h}{\partial y^2}+\frac{\partial^2 h}{\partial z^2}=\frac{S_s}{K}\frac{\partial h}{\partial t}+\frac{W}{K} \quad (2)$$

For a horizontal confined aquifer of thickness b, $S=S_s \times b$ and the transmissivity ($T= K_x \times b$), Eq. (2) becomes:

$$\frac{\partial^2 h}{\partial x^2}+\frac{\partial^2 h}{\partial y^2}+\frac{\partial^2 h}{\partial z^2}=\frac{S}{T}\frac{\partial h}{\partial t}+\frac{W}{K} \quad (3)$$

For a steady state flow, where $\frac{\partial h}{\partial t} = 0$, Eq. (3) becomes:

$$\frac{\partial^2 h}{\partial x^2}+\frac{\partial^2 h}{\partial y^2}+\frac{\partial^2 h}{\partial z^2}=\frac{W}{K} \quad (4)$$

According to Todd and Mays [2], finding an exact solution to Eqs. (2–4) is feasible only under highly idealized conditions. For practical purposes, some form of numerical approximation is typically necessary. One of the most widely used groundwater (GW) modeling packages is GMS MODFLOW. Numerical methods based on finite differences are utilized to solve Eqs. (1) to (4). To simulate and solve the steady-flow condition, a 3D finite-difference model was run using the GMS program. Establishing layers of flow domain, defining the boundary and initial conditions for the aquifer parameters, estimating the parameters, and ultimately calibrating the model to investigate the effects of the confined aquifer's actual recharge rates are part of creating a conceptual model. ArcGIS v10.8 is employed for geospatial analysis, visualization, and digital elevation model (DEM) processing, the digital elevation model (DEM), as shown in Fig. 1 (C). In Fig. 2, the methods employed in numerically modeling groundwater flow in the selected study area are presented. The process of model conceptualization involves systematically identifying coverage to describe field conditions, including sources/sinks and boundary conditions. Areal properties are utilized to define the top and bottom elevations of the aquifer layers, as well as aquifer properties such as discharge rate and HK for steady-state simulation. Observation points are employed to define the observation well point, represented as (head), in the static or steady-state case. The necessary coverages are created to accurately depict the groundwater flow processes in the modeled area. Once all coverages are completed, the conceptual model is converted into a 3D grid model.

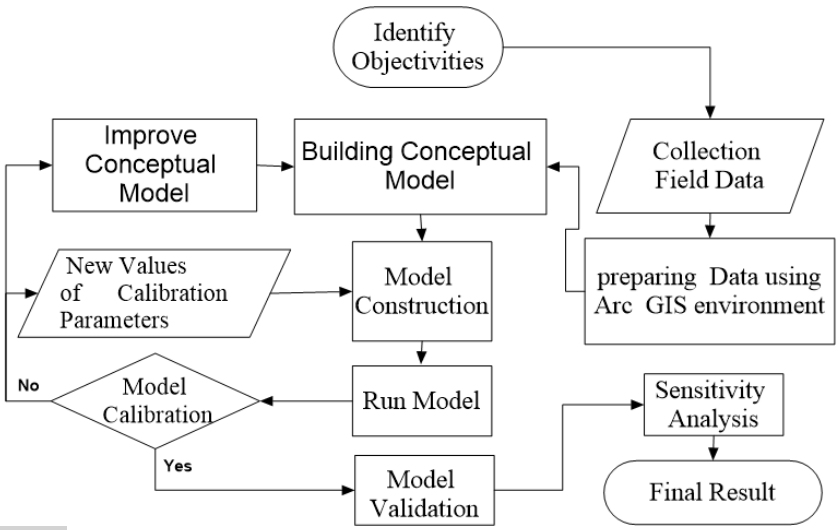

Fig. 2 Methodology of the Simulation Processes by GMS MODFLOW.

3.GRID DESIGN

A 3D finite-difference cell-centered grid consisting of 100 rows and 100 columns was created using the MODFLOW package, integrated with the GMS program. The cell sites are defined by their respective rows (I), columns (J), and layer numbers (K). The modeled domain comprised 10,000 cells, each with dimensions of 2959 × 2317 m and a thickness of 300 m, as depicted in Fig. 3. Of these, 3259 were active cells, and 6741 were inactive cells. Each cell was compared to the coverage polygons, as shown in Fig. 3. A cell was considered to be outside the model's domain if any of the polygons did not contain it, while cells inside the domain were classified as active cells (https://xmswiki.com/wiki/GMS:GMS_User Manual_10.4).

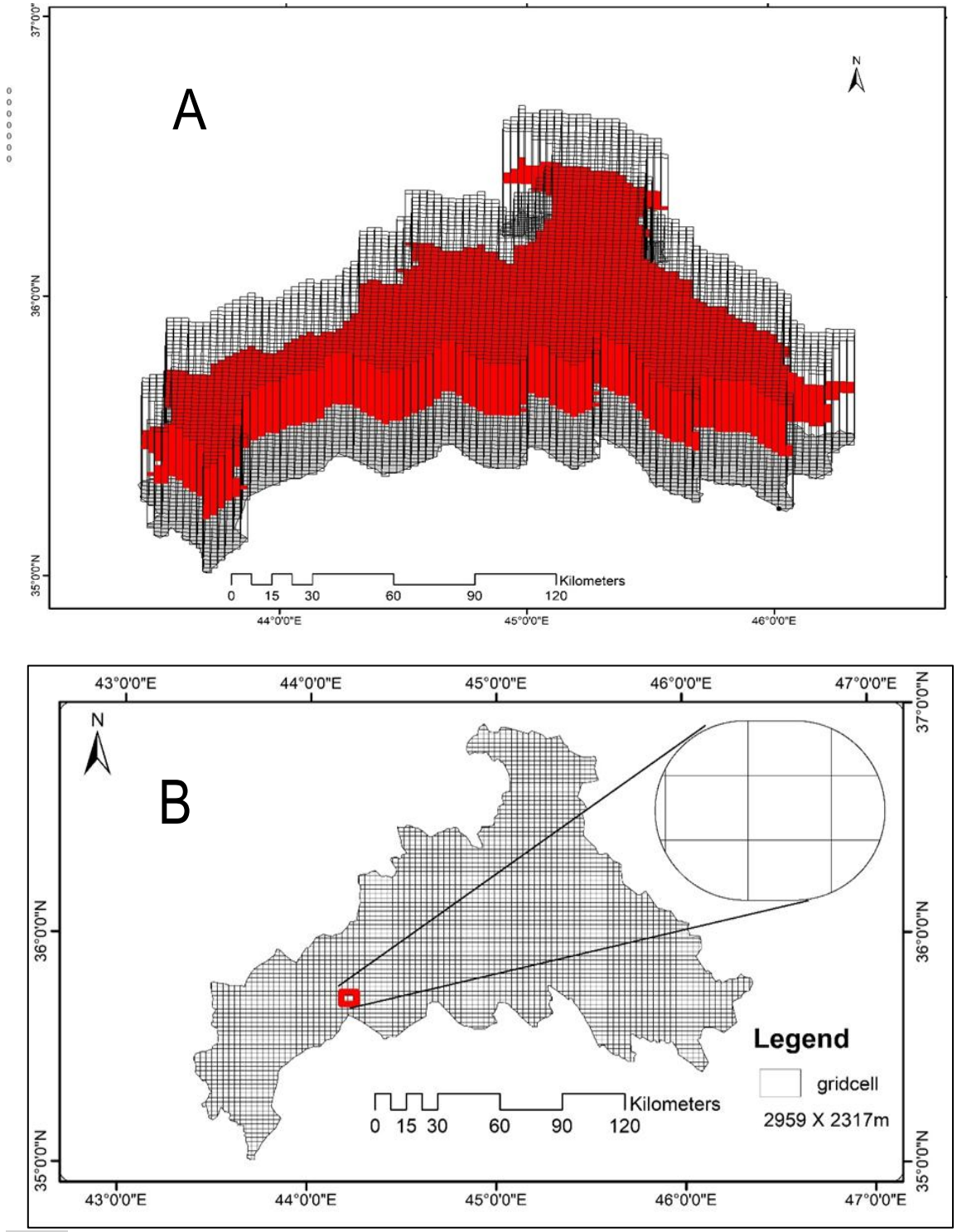

Fig. 3 (A) Three-Dimensional Grid Established for the Lower Zab River Basin with Z Magnification Set to 30. (B) Two-Dimensional Grid for Active Cells.

4.BOUNDARY AND INITIAL CONDITIONS

Based on the regional groundwater flow pattern of the study basin confined aquifer, a constant-head boundary (CHD) was created in the groundwater well field to regulate the influence on simulated heads within the model domain. Figure 1 (B) and Table 2 depict that the Tigris River is an arc with distinct endpoints or nodes. The General Committee for Groundwater/Ministry of Water Resources, Iraq, provided the riverhead and bottom elevations for each node. 0.0004 was chosen as the area's recharge after the constant head and recharge constant head values were determined using the observation wells. The term "unit hydraulic conductivity" refers to a medium's ability to transfer a unit volume of groundwater at the dominant kinematic viscosity (V) in a unit amount of time through a cross-section of the unit area measured at right angles to the flow direction under a unit hydraulic gradient. In groundwater hydrology, where water is the predominant fluid, hydraulic conductivity (k) is helpful for practical work:

$$K = \frac{\boldsymbol{v}}{\mathbf{dh}/\boldsymbol{dl}} = \boldsymbol{m/day} \qquad \textbf{(5)}$$

In its natural condition, groundwater is continually flowing. The established hydraulic principles control this movement. Flow through aquifers, which are predominantly naturally permeable, is described by Darcy's law. One crucial variable in the flow equation is hydraulic conductivity, which measures the medium's permeability. Multiple field or laboratory techniques are available to determine hydraulic conductivity. Typically, groundwater flow rates and directions are estimated using Darcy's law. According to Mirlas et al. [18], differences in hydraulic conductivity and specific storage values within the first-order values (±10 times) did not significantly affect the estimated groundwater levels because there are several ways to assign HK to the groundwater model in GMS. HK was assigned to polygons within a single coverage using the MODFLOW model-mapping technique and a conceptual model. As illustrated in Fig. 4, the study area was segmented into five zones to determine the initial HK values. For estimation purposes, the GMS software uses the inverse model tool (PEST). A user-defined initial set of input parameters (HK and RH) is gradually adjusted until the difference between the calculated and observed values is minimized. This process begins with inputting the initial HK values, which, as shown in Fig. 4, were sourced from the General Committee for Groundwater/Ministry of Water Resources, Iraq. According to earlier research, Mustafa et al. [19], the different recharge rates in the modeling instance range from about 15% to 40% of the region's normal annual rainfall. A starting point of 5% of the average daily rainfall was recommended for the RH [17]. As a result, the initial RHs for the governorates under study have been set at 0.00035 and 0.0004 m/day. Since the differences in computed recharge values across the governorates under study are negligible, the study region was considered a single zone with an initial recharge rate of 0.0004 m/day. Groundwater recharge occurred during the rainy season, which ran from November to June, with daily and annual fluctuations due to land use, soil types, precipitation temporal distribution, and annual variations in precipitation rate [20]. In Sulaymaniyah Province, the annual weighted-average of groundwater recharge was 105.8 mm/year, or 17.6% of the average annual precipitation of 602 mm/year, while evapotranspiration accounted for 69.4% of the loss.

5.STATISTICAL CRITERIA

5.1.The Normalized Root Mean Squared Error (NRMSE)

A model's accuracy is measured by the NRMSE of its predicted values compared to its observed values, normalized by the observed range, mean, and standard deviation. Using this method, the performance of different models across datasets can be compared in a standardized manner.

$$\textbf{RMSE} = \frac{\sum(H_s - H_o)^2}{\sum H_o^2} \qquad \textbf{(6)}$$

where H_s are observed values, and H_o are simulated values.

5.2.The Root Mean Squared Error (RMSE)

$$\textbf{RMSE} = \sqrt{\frac{\sum(H_s - H_o)^2}{n}} \qquad \textbf{(7)}$$

5.3.The Standard Error (SE)

$$\textbf{SE} = \frac{\sigma}{\sqrt{n}} \qquad \textbf{(8)}$$

$$\sigma = \sqrt{\frac{\sum(H_o - \bar{H}_O)^2}{N}}$$

where N is the number of data.

5.4.Mean Absolute Error

$$\textbf{MAE} = \frac{\sum|H_s - H_o|}{n} \qquad \textbf{(9)}$$

If the RMSE is less than a predetermined percentage of the calibration target range, the model may be deemed adequately calibrated. In other words, using 10% as a criterion, an acceptable RMSE is around 10 m if the head targets are between 50 and 150 m. However, there is no logic to back up the claim that a model is suitably calibrated just because it satisfies this requirement. Other than the fact that it is preferable to minimize these values, there are no set industry standards for the permissible magnitude of the ME, MAE, or RMSE. The modeling community has not adopted standardized calibration criteria, despite acknowledging their usefulness. This neglect partly reflects the understanding that any modeling requires subjective assessment [15].

Table 2 Boundary Conditions Values of the Rivers for The Simulated Region.

River	Location			River	
				Stage	Bed
	Name	x	Y	m.a.s.l	m.a.s.l
Lesser Zab	Upstream / Near Dokan	500876.5	3984086	560	554
	Downstream / Near Tigris	360727.1	3901536	254	250

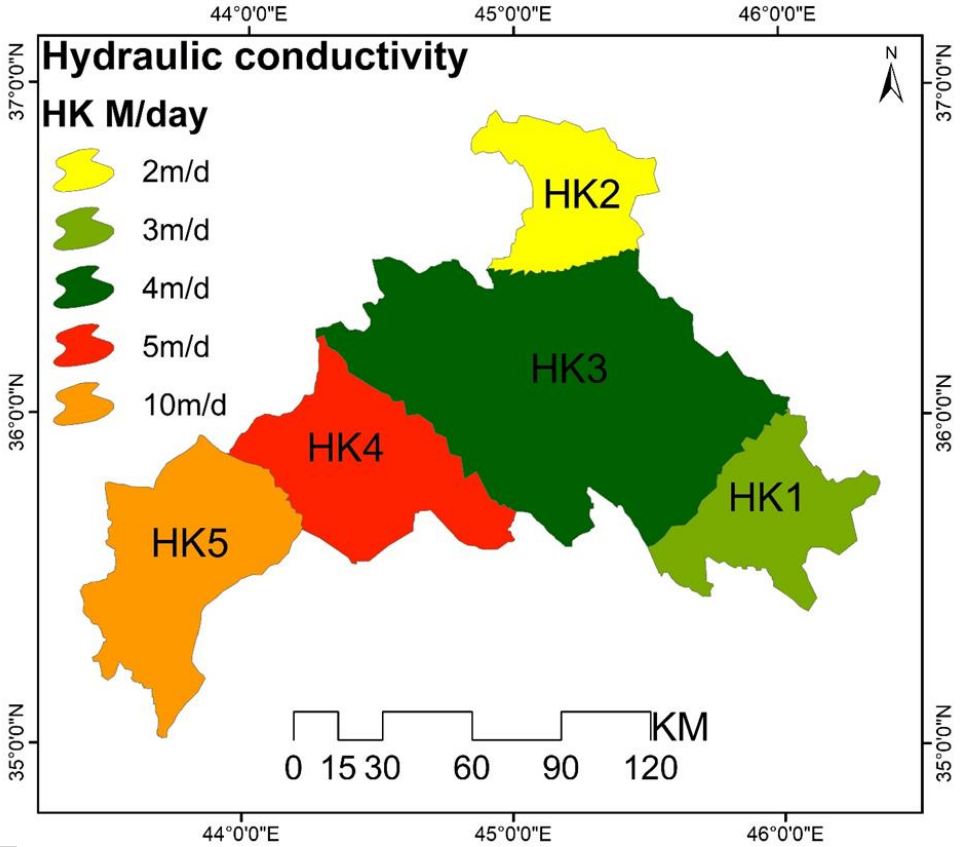

Fig. 4 The Initial Hydraulic Conductivity Zones (in M/Day) for The Lower Zab River Basin.

6.RESULTS AND DISCUSSION

The simulation of the groundwater head in the watershed indicates that the flow is from the north and northeast to the south and southwest, towards the lower Zab River. Furthermore, there is a flow from south to north and northwest, with regional variations depending on the watershed's geology and textural features. Hydraulic continuity exists between water-bearing formations within these zones, depending on the piezometric relations of the water-bearing layers throughout the area. Groundwater flow can support 14-38% of the basin's flow in the Lower Zab River watershed. Due to differences in the drainage area for each sub-basin, as well as the presence of aquifers with larger releases in the downstream location than the upstream one, there were comparatively significant differences in the baseflow contributions between the upstream and downstream sub-basins [7]. During calibration, the computed and observed values are automatically compared. After the model was calibrated for the thirty observation wells, the average and simulated groundwater levels were compared. The most sensitive parameters, including hydraulic conductivity, recharge, and conductance for the river and reservoir, were manually adjusted within acceptable ranges through trial and error to minimize the differences between computed and measured heads. This study found that changing the conductance values significantly impacts the head value. Recharging, on the other hand, strongly affected and considerably altered the head value, but it was less significant than the conductance. The hydraulic conductivity had a limited and negligible impact compared to recharge. Additionally, any alteration to a specific head is on the side of the determinants. Despite its massive impact, the layer is insignificantly affected by its thickness or distance from the Earth's surface. In a similar vein, the amount of water extracted depends on its distribution, frequency, and withdrawal times. A 95% confidence interval and a 5 m permitted head interval were used to compute the residual values. The estimate's standard error is 0.625 m, its root mean square is approximately 3.531, its NRMS is -3.35, and its maximum and minimum residuals are 5.532 m in W_8 and -7.25 m in W_4, respectively. The sudden high draft that occurs in the measurement area may cause a reading of the water level at an inappropriate time for measurement, or the extremes of this reading

when it is affected by the neighboring area—which was excluded from the modelling because the study area is confined to borders—may be the cause of the presence of such abnormal values. Uncertain and unable to be infinitely open. Furthermore, this reading could not be excessive or unusual because of the designer's rigorous modelling constraints. Particularly in mountainous regions where steep hillsides meet deep valleys next to them, several studies and publications indicate permittivity exceeding 10 m, as demonstrated by Yogendra Sharma's 2024 research. The residual and absolute residual means are -1.053 m and 2.98 m, respectively. The comparison results indicate a correlation coefficient of 0.999. However, Fig. 5 provides a detailed explanation of the comparison of measured and simulated groundwater heads.

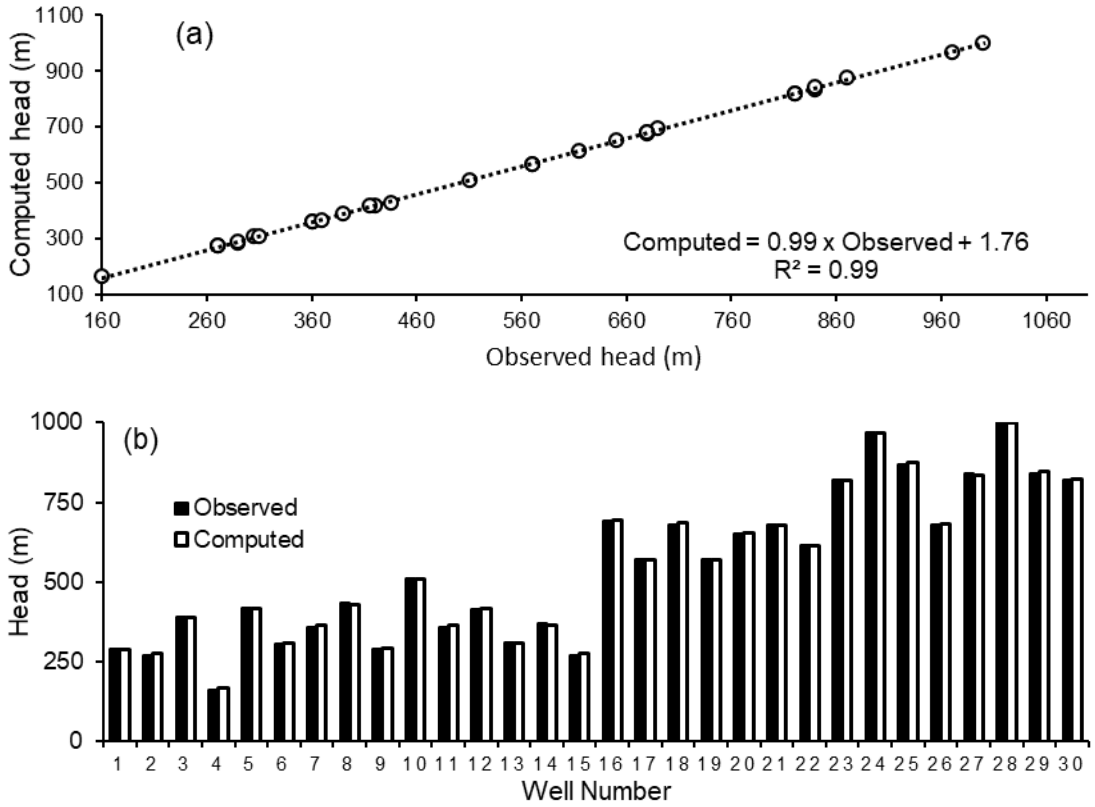

No. of data points: 30
Max Residual: 5.5 M, at W8
Min Residual: -7.25, at W4
Residual Mean: -1.05m
Abs Residual Mean: 2.98
95% confidence
Standard Error of the Estimate 0.625.
Root Mean Squared: 55
Normalized Root Mean Square R MS: -3.35
Correlation Coefficient:0.999
5m interval

Fig. 5 Comparison of Measured and Simulated Groundwater Head (M A. S. L) at The Confined Aquifer Condition.

The contour map of the aquifer's simulated piezometric heads is shown in Fig. 6. Green error bars represent 24 of the 30 observation targets in the steady-state simulation. It was found that the values for two of the observation target wells exactly match the observed values. Although there were only four yellow error bars, they were discovered to be within the allowed bounds of the targets, which was a notable improvement over the initial findings. The HK, RH, and flow direction were all determined. The aquifer appears as a single layer that has developed in a small area and is 300 m thick. The Mean Error)ME(, Mean Absolute Error)MAE(, and Root Mean Square Error)RMSE(were used to evaluate the model's dependability. The RMSE represents the average of the squared residuals, while the ME indicates the difference between the residual errors, and the MAE signifies the mean of the residual's absolute value [15]. ME, MAE, and RMSE are -1.053 m, 2.982 m, and 3.53 m, respectively. Since the head calibration target is set at 5 m and the calculated RMSE is 3.53 m, these statistical measures indicate that the conceptual model, boundary conditions, and final hydrological parameters were reasonable and usable. Figure 7 displays the statistical error measures for the steady-state calibration. Table 3 shows that the residual head values, representing the discrepancy between the estimated and observed head, were below the permitted error limit of 5 m.

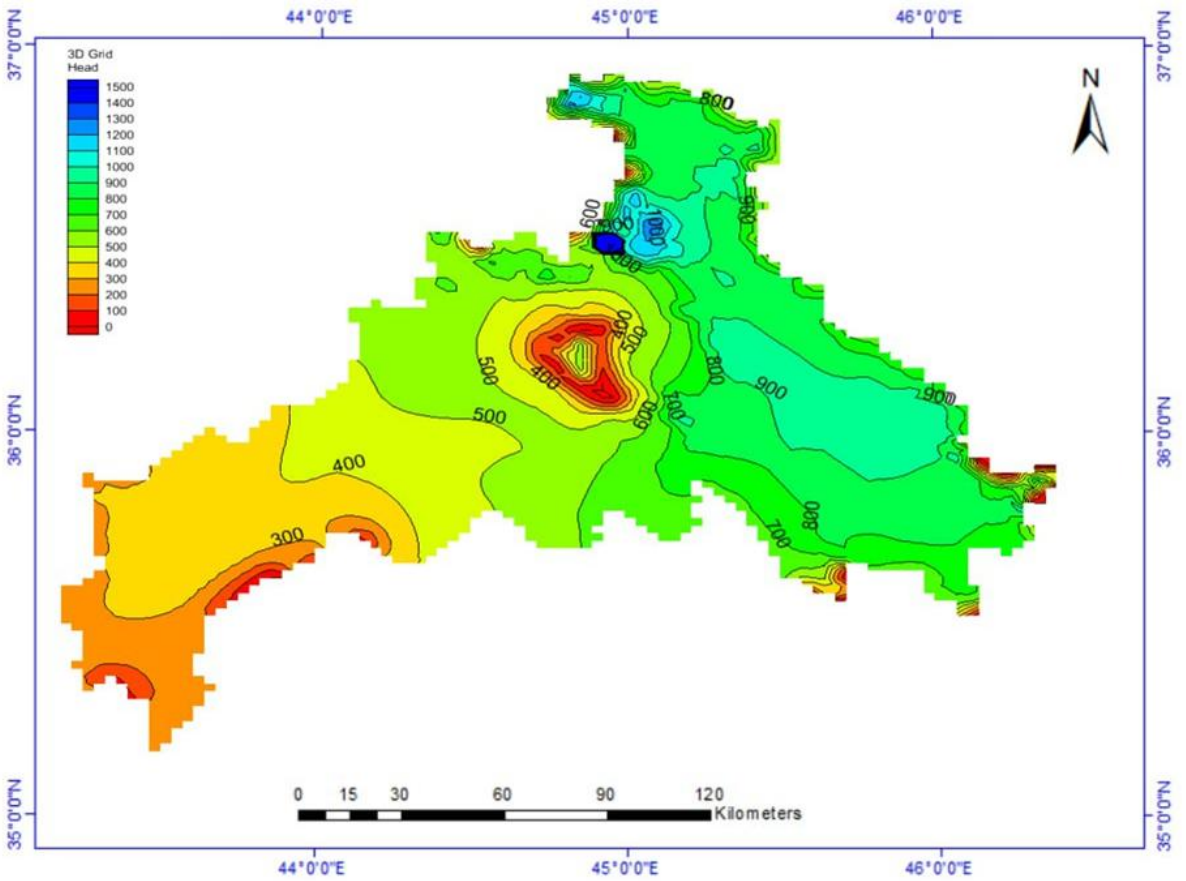

Fig. 6 Contours Map with The Simulation Piezometric Head (M).

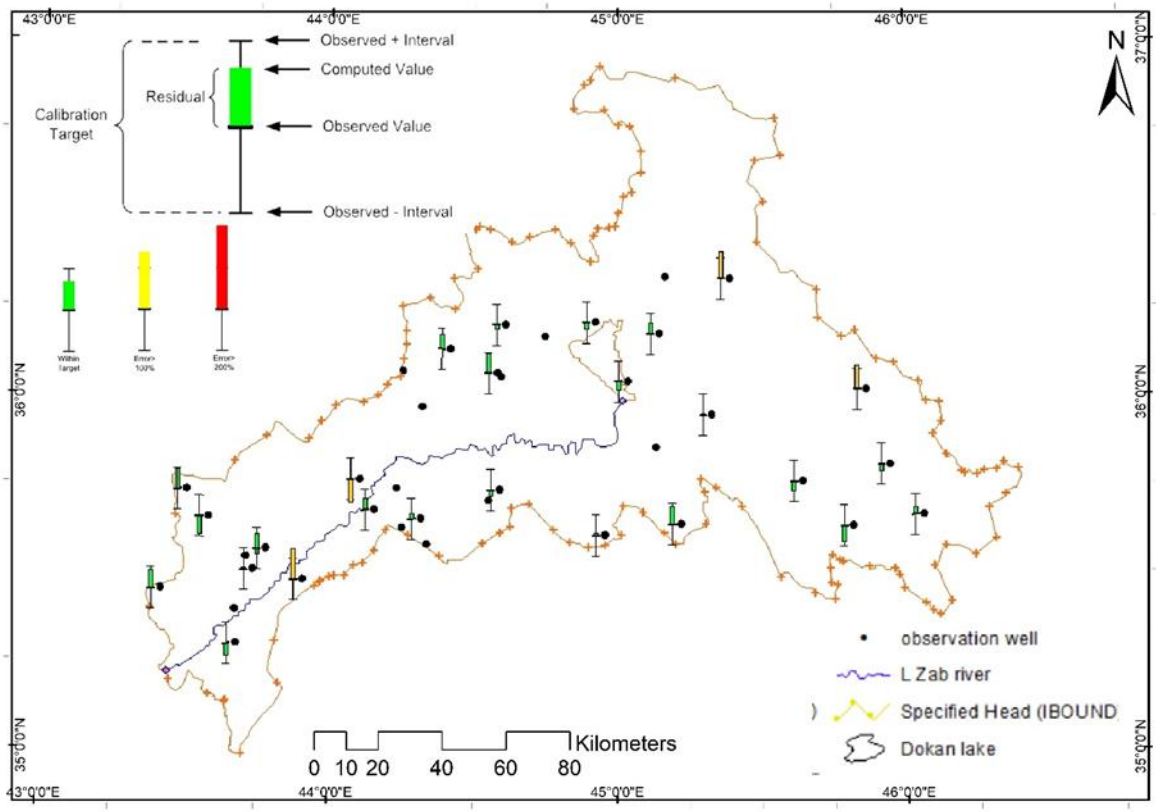

Fig. 7 Statistical Error Measure Utilized for Calibration.

Table 3 Observed, Simulated, and Residual Head During the Calibration Process for the Period (2014-2015).

Well number	Head (m)			Well number	Head (m)		
	Observed	Simulated	Residual		Observed	Simulated	Residual
W_1	290	286.95	3.05	W_{16}	690	694.71	-4.71
W_2	270	274.35	-4.35	W_{17}	570	568.45	1.55
W_3	390	390.17	-0.17	W_{18}	680	684.34	-4.34
W_4	160	167.25	-7.25	W_{19}	570	568.04	1.96
W_5	420	418.41	1.59	W_{20}	650	653.47	-3.47
W_6	305	309.62	-4.62	W_{21}	680	679.06	0.94
W_7	360	362.69	-2.69	W_{22}	615	615.53	-0.53
W_8	435	429.47	5.53	W_{23}	820	818.32	1.68
W_9	290	291.13	-1.13	W_{24}	970	967.47	2.53
W_{10}	510	508.65	1.35	W_{25}	870	875.62	-5.62
W_{11}	360	362.69	-2.69	W_{26}	680	681.56	-1.56
W_{12}	415	418.41	-3.41	W_{27}	840	835.92	4.08
W_{13}	310	309.62	0.38	W_{28}	1000	1000.27	-0.27
W_{14}	370	365.71	4.29	W29	840	846.65	-6.65
W_{15}	270	274.35	-4.35	W30	820	822.72	-2.72

Figure 8 demonstrates the agreement between the modelling results and field observations. The model indicates a strong correlation between computed and observed water levels and clearly displays the residuals and their values for each well.

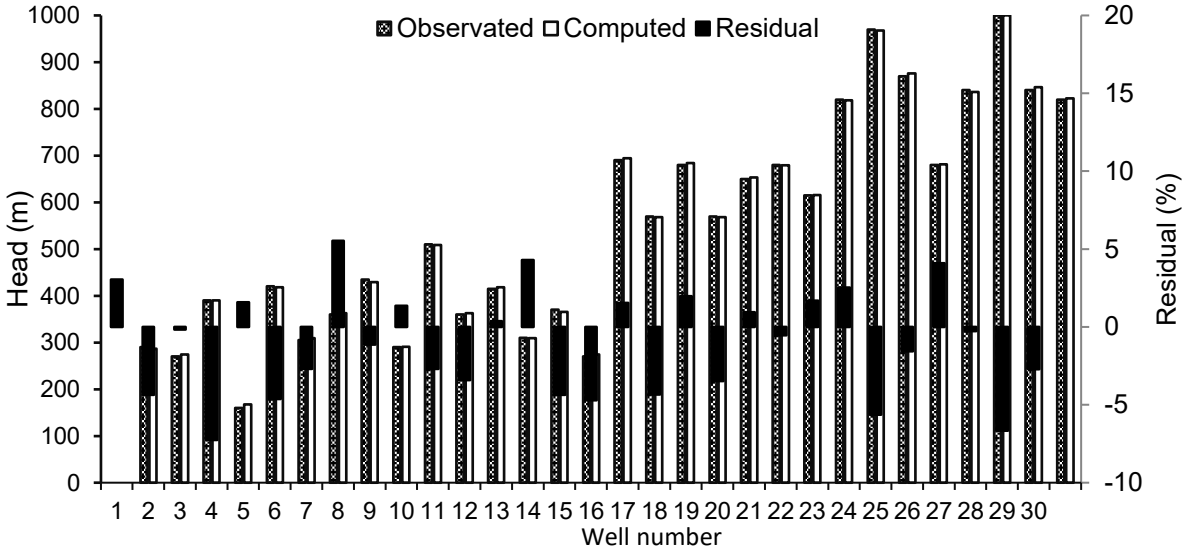

Fig. 8 Observed, computed, and residual head for each observation well in the Lower Zab River Basin.

7.CONCLUSIONS AND RECOMMENDATIONS

Using the Groundwater Modelling System (GMS V10.7), this study examines the stresses and potential for degradation affecting the limited aquifer in the Lower Zab watershed across the governorates of Sulaymaniyah, Erbil, and Kirkuk. The estimated recharge rate (RH) was 0.0004 m/day, while the steady-state calibration indicated a hydraulic conductivity (HK) of 3-10 m/day. Each of the watershed's 30 observation wells was calibrated using a model that compared simulated and observed groundwater heads. The characteristics with the lowest residual were recharge, hydraulic conductivity, and conductance (for rivers and reservoirs), which were discovered to be the most sensitive. The model's reliability was evaluated using ME, MAE, and RMSE. The estimate's ME is 0.6259 m; its RMSE is roughly 3.531 m; its normalized root mean square (RMS) is -3.352; and its residual mean and absolute residual mean are -1.053 m and 2.982 m, respectively. The maximum and minimum residuals are 5.532 m in well W_8 and -7.254 m in well W_4. The correlation coefficient for the comparison results is 0.999. The simulation of groundwater head indicates a predominant flow direction from the north and northeast towards the southern and southwestern regions, ultimately leading to the Lower Zab River, based on the watershed's geological and textural features. Additionally, there is a flow from the south towards the north and northwest, with localized variations in direction. The piezometric relationships of the water-bearing layers in the area establish the hydraulic continuity among the water-bearing formations within these zones. Moreover, the simulation advocates that the head originates in the northeastern section of the plain, descending from 1000 m above sea level to 160 m in the south.

ACKNOWLEDGEMENTS

The authors are grateful for the financial support towards this research by the Civil Engineering Department, College of Engineering, Babylon University. Postgraduate Research Grant (PGRG) No.TU.G/2020/HIR/MOHE/ENG/16140.

NOMENCLATURE

A	Area, km^2
g	Gravitational constant, m/s^2
HK	Horizontal hydraulic conductivity, m/day
h	Hydraulic head (m)
i	Hydraulic gradient (L/T)
k	Hydraulic conductivity, m/day
L	Length, m
RH	Recharge rate m/day
S	Storage coefficient
Ss	Specific storage (L^{-1})
t	Time
T	Transmissivity m^2/s
W	Volumetric flux per unit volume
Subscripts	
DEM	Digital Elevation Model
GMS	Groundwater Modeling System software
IDW	Inverse Distance Weighted method
m.a.s.l	Meter above sea level
SRTM	Shuttle Radar Topography Mission
MAE	Mean Absolute Error
GIS	Geographic Information System
ME	Mean Error
Modflow	Modular Finite -Difference Flow Model
MSE	Mean Square Error
Pest	Parameter estimation process program
RMSE	Root mean square error
UTM	Universal Transverse Mercator

REFERENCES

[1] Al Zubedi AS. **Groundwater in Iraq.** 1st ed., Baghdad: Araa Publication; 2022.

[2] Todd DK, Mays LW. **Groundwater Hydrology.** 3rd ed., USA: John Wiley & Sons; 2005.

[3] Abbas SA, Xuan Y, Bailey RT. **Assessing Climate Change Impact on Water Resources in Water Demand Scenarios Using SWAT-MODFLOW-WEAP.** *Hydrology* 2022; **9**(164): 2–24.

[4] Khayyun TS, Mahdi HH. **Estimation of Average Groundwater Recharge by Using Groundwater Modelling System (GMS) Program for Upper Zone of Iraqi Aquifers System.** *Journal of Critical Reviews* 2020; **7**(09): 3094–3112.

[5] Khatiri KN, Nematollahi B, Hafeziyeh S, Niksokhan MH, Nikoo MR, Al-Rawas G. **Groundwater Management and Allocation Models: A Review.** *Water* 2023; **15**(2): 253.

[6] Mustafa JS, Mawlood DK. **Mapping Groundwater Levels in Erbil Basin.** *American Scientific Research Journal for Engineering, Technology, and Sciences* 2023; **93**(1): 21–38.

[7] Mohammed R, Scholz M. **Flow–Duration Curve Integration into Digital Filtering Algorithms for Simulating Climate Variability Based on River Baseflow.** *Hydrological Sciences Journal* 2018; **63**(10): 1558–1573.

[8] Al-Gburi HF, Al-Tawash BS, Al-Tamimi OS, Schüth C. **Impacts of Hydrogeochemical Processes and Land Use Practices on Groundwater Quality of Shwan Sub-Basin, Kirkuk, Northern Iraq.** *Heliyon* 2023; **9**(3): 1–20.

[9] ALSlevani IN, ALMohsen KA. **Integrated Application of (MODFLOW) and (WEAP) Model in Nineveh Province.** *Journal of University of Duhok* 2017; **20**(1): 690–700.

[10] Ta'any RA, Al-Arabiyat A, Mahameed J, Al–Zu'bi J. **Groundwater Management Using MODFLOW Model in Jerash Catchment Area/Jordan.** *Assiut University Bulletin for Environmental Researches* 2013; **16**(2): 113–138.

[11] Baghel T, Sinha MK, Verma MK, Ahmad I. **Modeling Groundwater Flow in Upper Seonath Basin, Chhattisgarh, India.** *Ecology Environment and Conservation* 2018; **24**(1): 292–298.

[12] Marios K. **Simulation of Groundwater Flow Using the MODFLOW Code in the Alluvial Aquifer of Korisos Basin.** *M.Sc. Thesis, Aristotle University* 2015.

[13] Sissakian VK, Khadim TH, AbdulJabbar MF. **Geomorphology of the High Folded Zone.** *Iraqi Bulletin of Geology and Mining* 2014; **1**(6): 7–51.

[14] Yacoub SY, Othman AA, Kadhim TH. **Geomorphology of the Low Folded Zone.** *Iraqi Bulletin of Geology and Mining* 2012; **1**(5): 7–37.

[15] Anderson MP, Woessner WW, Hunt RJ. **Applied Groundwater Modeling: Simulation of Flow and Advective Transport.** 2nd ed., U.S.A: Academic Press; 2015.

[16] US Geological Survey. **EarthExplorer.** 2023.

[17] Aquaveo. **The Groundwater Modeling System (GMS) User Manual, Version 10.4.** 2018.

[18] Mirlas V, Zhakyp A, Auelkhan Y, Anker Y. **Assessment of Urbanization Related Groundwater Flooding Process via Visual MODFLOW Modeling: A Case Study for the Northern Part of Almaty City, Kazakhstan.** *Journal of Flood Risk Management* 2024; **e13029**: 1–20.

[19] Mustafa JS, Mawlood DK. **Assessment of the Groundwater in Erbil Basin with Support of Visual MODFLOW.** *Journal of Ecological Engineering* 2024; **25**(4): 203–227.

[20] Ghafur PG. **Assessment of Spatial and Temporal Variability of**

Groundwater Recharge in Sulaimani Province, Iraqi Kurdistan. *Doctoral Dissertation, Department of Geography, University of Leicester* 2013.